Time Series of Daily Averaged Cloud Fractions over Landfast First-Year Sea Ice from Multiple Data Sources

XIN JIN, JOHN M. HANESIAK, AND DAVID G. BARBER

Centre for Earth Observation Science, University of Manitoba, Winnipeg, Manitoba, Canada

(Manuscript received 13 April 2006, in final form 7 February 2007)

ABSTRACT

The time series of daily averaged cloud fractions (CFs) collected from different platforms—two Moderate Resolution Imaging Spectroradiometer (MODIS) instruments on *Terra* and *Aqua* satellites, the National Centers for Environmental Prediction (NCEP) model, a Vaisala 25K laser ceilometer, and ground-based manual observations (manobs)—above the winter camp of the Canadian Arctic Shelf Exchange Study (CASES) field experiment are analyzed in this study. Taking the manobs as standard, the authors conclude that 1) the NCEP products considerably underestimated CFs in spring (e.g., from April to May) and 2) the performance of two MODIS products depends on the variation of solar zenith angle (SZA). *Aqua* MODIS misrepresents the snow-covered surface as clouds with almost randomly distributed CFs during the dark winter [cos(SZA) $<$ 0], leading to the overestimation of CFs in winter while *Terra* MODIS has good agreement with manobs. When $0.1 < \cos(\mathrm{SZA}) < 0.4$, both MODIS products regularly misrepresent the snow-covered background as clouds, leading to the significant overestimation of CFs in late winter (February) and early spring (March). When cos(SZA) $>$ 0.4, both MODIS products have good performance in detecting cloud masks over snow backgrounds. If the sky is slightly cloudy, surface-based meteorological observers tend to underestimate cloud amounts when there is a lack of light. Comparing the CFs from *Terra* and manobs, the authors conclude that this bias can be over 10%. Power spectral analysis and wavelet analysis show three results: 1) High clouds more frequently appear in winter than in spring with periods between 8 and 16 days, indicating their close connection with synoptic events. Current NCEP products can predict this periodicity but have a phase lag. 2) Middle and low clouds are more local and are common in mid- and late spring (April and May) with periods between 2 and 4 days. At the CASES winter and spring field site, the periodicity of high clouds is dominant. 3) The time-scale-dependent correlation coefficients (CCs) between both MODIS products, NCEP and manobs, show that with high frequent CF sampling per day, the CCs are stable when the time scale varies between 1 and 4 days: with *Terra* MODIS and NCEP, the value is about 0.6; with *Aqua* MODIS, between 0.4 and 0.5. All CCs get smaller when the time scale increases beyond 8 days: with respect to both MODIS products, the CCs get closer with values between 0.3 and 0.4; with respect to NCEP, the CC dramatically decreases from positive values to negative values, indicating the lack of accuracy in current NCEP cloud schemes.

1. Introduction

Clouds are critical in the Arctic climate system because of the control they have on radiative exchange with the surface (Curry et al. 1996; Walsh and Chapman 1998; Minnett 1999). Detection and measurement of cloud parameters, either in situ or from space, remain a challenge. The basic statistical properties of clouds are relatively poorly known throughout the annual time–space cycle over sea ice because of the difficulty in mounting field programs in these regions. The intercomparisons between different satellite databases and ground-based validations in the Arctic region are required if we want to make such studies meaningful. With some validation studies (Schweiger et al. 1999, 2002; Key et al. 2004) we now know that International Satellite Cloud Climatology Project (ISCCP) D series cloud amount data differ significantly with surface observations while Television and Infrared Observation Satellite (TIROS) Operational Vertical Sounder (TOVS) related cloud fractions are better related to ground observations at a time scale of greater than 4 days (correlation coefficient $>$ 0.7). Key et al. (2004) also confirm that 95% scenes have multiple cloud types,

Corresponding author address: Xin Jin, Faculty of Environment, University of Manitoba, Winnipeg, MB R3T2N2, Canada. E-mail: umjinx@cc.umanitoba.ca

DOI: 10.1175/2007JAMC1472.1

the majority of which are midlevel ice cloud and low-level liquid cloud. They still find that despite large discrepancies in diurnal cloud amount, regional averages of ISCCP pixel cloudiness over the length of the experiments agree within ±5% of surface observations. These conclusions remind us that temporal scales and spatial resolutions of satellite datasets can be crucial in ground validation studies.

The Moderate Resolution Imaging Spectroradiometer (MODIS) provides a means to obtain cloud amount data in high-latitude areas with high spatial and temporal resolution (1 km and 1.5 h). Ground validation for cloud amounts from two MODIS instruments on *Terra* and *Aqua*, respectively, has previously been reported for different Arctic sites. Li et al. (2004) evaluated MODIS cloud fractions with data from a whole sky imager (WSI) at the North Slope of Alaska (NSA), concluding good agreement between the two cloud fractions. Li et al. (2004) also point out that at the NSA, the MODIS overestimates the cloud fraction under clear-sky conditions with snow backgrounds and they think this resulted from various issues with different algorithms (Ackerman et al. 1998). The WSI can only work in the presence of sunlight, so these results are limited to these time periods. The validation of MODIS cloud amounts at night in polar areas shows that current cloud detecting tests need more improvement (Liu et al. 2004).

The consistency of data quality between two MODIS instruments has not been widely studied. Minnis et al. (2003) point out that cloud properties from both MODIS products agree well in most areas on the earth except some high-latitude areas, and the cloud amount is one of those properties included that is explained as diurnally dependent changes in the clouds. In this study, we will make a ground calibration of the consistency of cloud fractions (CFs) between two MODIS instruments at a coastal site, over landfast first-year sea ice in the Beaufort Sea during the winter and spring seasons. Since the study based on CFs from the National Centers for Environmental Prediction (NCEP) model differ from those based on the TOVS Polar Pathfinder (Path-P) dataset (Chen et al. 2002; Schweiger 2004), the CFs from NCEP will also be evaluated in this study.

2. Data and methods

The winter camp of the Canadian Arctic Shelf Exchange Study (CASES) was located over landfast first-year sea ice in Franklin Bay (70.03°N, 126.18°W) of the Beaufort Sea from 22 November 2003 to 31 May 2004. MODIS cloud mask products were collected from the

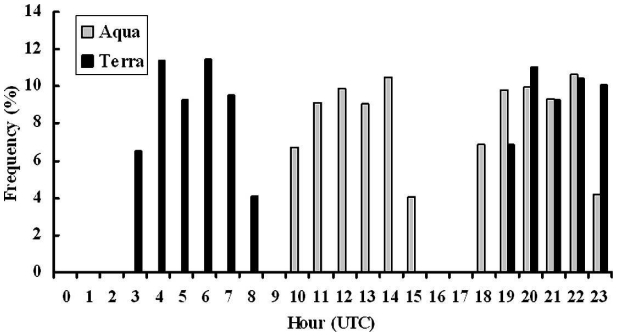

FIG. 1. Frequencies of MODIS overpassing the CASES winter camp within a day.

MODIS Atmosphere Level-2 Joint Product, version 4, which contains a spectrum of key parameters gleaned from the complete set of standard at-launch level-2 products. Note that the MODIS cloud mask products discussed in this paper were collected in 2004 and Liu et al.'s (2004) improvements on MODIS night cloud detection have not been involved. The CF in this level-2 joint product has a spatial resolution of 5 km, which is subsampled from the original 1-km-resolution level-2 cloud mask product by simple averaging. For each granule we calculate the average value of all CFs from those pixels centered at the campsite and within a radius of 20 km as the average CF detected by MODIS in this granule. Then we average all CFs from all of the tracks that overpass the study site each day as the daily averaged CF by MODIS. Figure 1 shows the frequencies of MODIS granules covering the study area within an average day. The period at which the 2 satellites overpass the camp is within 30 min from 1900 to 2400 UTC [1300 to 1800 local standard time (LST)]. This is coincident with the time for which surface observations are also available, which means the diurnally dependent changes are minimized so that the comparison of the consistency between two MODIS sensors is possible.

Manual observations were conducted hourly, in general, between 0800 and 2300 LST (i.e., 6 h behind UTC). A Vaisala CT25K laser ceilometer was set up to measure the cloud-base height (CBH) or vertical visibilities with a temporal resolution of one minute. A dataset of daily CF from this unit was then generated by counting the percentage of cloud-detected events out of all events within a particular day. An advantage of this unit is that it can work continuously and provide cloud information missed by observers. The cloud-base height from this ceilometer is used to determine cloud types by observers. In dark winter nights, it also helped observers to determine the existence of cloud above the study site. However, it has been found that high, very

visible cirrus clouds (above 6 km) were consistently undetected by the unit both in this field experiment and in an earlier study (Hanesiak 1998). This caveat provides a cloud-type detection scheme by comparing ceilometer and manobs datasets. Before applying this scheme, we have to minimize the sampling mismatch between these two datasets. According to weather records, from 22 November 2003 to 13 May 2004, there was only one observer on duty. The observer recorded cloud conditions hourly between 0800 and 2300 LST. From 14 May to the end of the May 2004, 2 observers were available so that the cloud condition was recorded 24 h per day. Note that the ceilometer was running all the time except for maintenance. This configuration means that there was a 9-h gap per day between these two datasets in the most of the field stage. We only selected the ceilometer measurements obtained between the manual observation spans to conduct our cloud-type detection scheme. This scheme resulted in an inevitable question: how to justify the impact of cloud variation between the 9-h gap. We admit that we do not have any technique to quantitatively evaluate this impact. This is a caveat in our study. However, the high temporal correlation in cloud fraction time series may help to lower the uncertainty. The World Meteorological Organization (WMO) recommended frequency of standard meteorological observation is 4 times per day (i.e., each observation is representative of the cloud conditions during the 3 h before and after the observation). Considering this criterion, our 0800-to-2300 observation was representative of the cloud conditions between 0500 on the current day and 0200 on the next day (LST). The temporal gap was minimized to 3 h in the early morning.

The result of the preanalysis in Fig. 2a shows the frequency distribution of CBH (km) from the ceilometer. Only 0.03% of all cloud-detected events by this unit have CBH higher than 6 km (high clouds are defined according to the WMO cloud classification code). So the CF dataset from this ceilometer mainly contains information of low clouds (CBH $<$ 2 km) and middle clouds (CBH between 2 and 6 km), and few high clouds with low CBHs. Figure 2b compares the frequencies of occurrence of different cloud types from manobs and the ceilometer. According to manobs, the frequencies of occurrence of low, middle, and high clouds are 46%, 25%, and 29%, respectively, but the ceilometer detected 22% middle clouds and almost all of the other clouds (77.99%) are low. Frequencies of occurrence of middle clouds from these two methods are well matched. This means that the main disadvantage of the ceilometer is inaccurate high-cloud sampling. If CFs from manobs are significantly larger than CFs from the

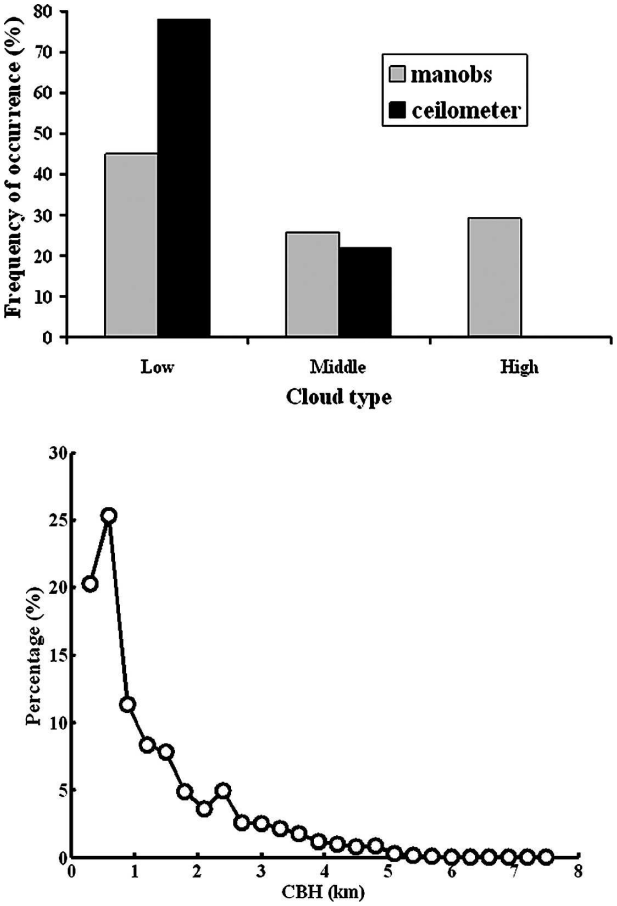

FIG. 2. (top) Frequency distributions of cloud types from manobs and ceilometer, and (bottom) the frequency distribution of cloud-base heights (km) from ceilometer.

ceilometer in a certain period, it is reasonable to say that the high clouds are more active within this period. Since the NCEP reanalysis, daily average CF data are in a T62 Gaussian grid and the selected grid is centered at (69.58°N, 126.00°W), the closest site to the CASES winter camp.

In this paper we use the wavelet analysis tools developed by Torrence and Compo (1998) to analyze the wavelet spectrums of CF time series. The wavelet base applied in this study is the Morlet function and the univariate lag-1 autocorrelation of the red noise background for each spectrum, according to the method recommended by Torrence and Compo (1998). It is calculated from $[\alpha_1 + (\alpha_2)^{1/2}]/2$, where α_1 and α_2 are the lag-1 and lag-2 autocorrelations of each CF time series. Other ancillary factors for applying the Morlet base are the same as those shown in the Table 2 of Torrence and Compo (1998).

The time scales of the correlations between the surface-based estimates and the satellite-based estimates

were widely used in evaluating satellite-based CF data quality (Schweiger et al. 1999; Schweiger et al. 2002). To evaluate CF datasets with surface observations at different time scales in this study, we will use the same discrete wavelet bandpass filter as they did. This method employs the maximum overlap wavelet decomposition (Lindsay et al. 1996) to obtain the wavelet coefficients of each time series using the Haar filter. An advantage of this method is that it provides information on the variability at a specific time scale and the variation at shorter and longer time scales can be filtered out, while the widely used smoothing average method can serve as a low-frequency filter.

3. Results and discussion

a. CF time series

The 10-day averaged CF time series between 22 November 2003 and 31 May 2004 is shown (Fig. 3). Taking CFs from manobs as the standard, the evolution of cloud amount in CASES agrees well with conclusions from other studies focused on Arctic environments (i.e., few clouds in winter and more clouds in spring; Intrieri et al. 2002; Walsh and Chapman 1998; Schweiger et al. 1999). The average CF quickly increases from around 0.4 to >0.7 with the major shift occurring between late April and early May. By comparing CFs from the ceilometer, we can observe that high clouds occur more frequently between mid-January and mid-April than over other periods in the time series, which may simply be due to them not being visible from the surface when low or mid-cloud becomes more extensive. This is similar to Curry and Ebert (1992) and lends support to the quality of the datasets used here. The NCEP CF time series, however, has a different pattern when compared with other data. All of the other four datasets agreed well and caught the dramatic increase of CF from late April (CF ≈ 0.4) to early May (CF ≈ 0.7) but NCEP CF remained near 0.2. Obviously, NCEP fails to catch the seasonality of Arctic cloud cover. Our finding is similar to Walsh and Chapman (1998), who compared CF from three databases: Russian drifting ice stations, NCEP reanalyses data, and the European Centre for Medium-Range Weather Forecasts (ECMWF). Recently, this caveat in NCEP is speculated to be due to the inaccuracy in predicting mixed-phased Arctic clouds (MPACs) in spring/autumn. Some unique dynamic and thermodynamic characteristics have been highlighted by recent studies to help understand the MPAC process (Fu and Hollars 2004; Zuidema et al. 2005; Shupe et al. 2005). From December to early April, the CFs from two MODIS instruments had different seasonal patterns relative to the manobs CF. In December and January, *Aqua* overestimated CFs relative to *Terra*, which agreed better with manobs. From mid-February to late March, both MODIS products significantly overestimated CFs (between 0.5 and 0.7) relative to manobs (CF varies between 0.2 and 0.4). According to the small values of CF from both manobs and the ceilometer, we can say that the cloudless or slightly cloudy skies are common during this period. Moreover, the obvious difference between CFs from the ceilometer and manobs indicates more high clouds in this stage. It is reasonable to assume that MODIS misrepresented the snow-covered background as clouds under clear or high-cloud events. However, after April, both MODIS products had very good agreement with manobs, indicating the good performance of MODIS cloud detection algorithms during the daytime. The monthly averaged CF deviations from the four databases in comparison with manobs are listed in Table 1.

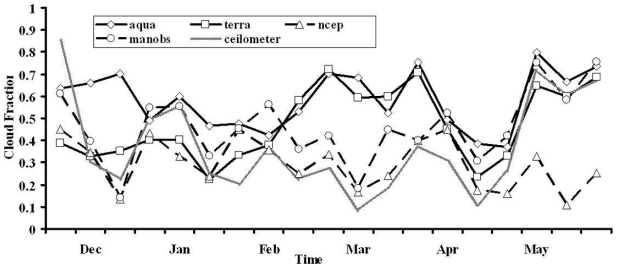

FIG. 3. The 10-day averaged CF time series between 22 Nov 2003 and 31 May 2004 from 5 datasets: *Aqua* (diamond), *Terra* (square), NCEP (triangle), manobs (circle), and ceilometer (gray line).

Here we take the manobs as standard to compare the performance of two MODIS instruments under clear and overcast skies. Before making the comparison, we address some points to explain why we choose manobs as standard instead of ceilometer for comparison with MODIS snapshots. We admit that relative to manobs, ceilometer measurement is more "objective." However, in CASES, because of the inability to detect high clouds, the benchmark of objective for ceilometer does

TABLE 1. Monthly average CF deviation from manobs.

Month	*Aqua*	*Terra*	NCEP	Ceilometer
Dec	0.25	0.00	−0.06	−0.02
Jan	0.07	−0.13	−0.11	−0.11
Feb	0.10	0.11	−0.13	−0.16
Mar	0.31	0.29	−0.08	−0.13
Apr	0.00	−0.08	−0.16	−0.19
May	0.04	−0.05	−0.47	−0.03

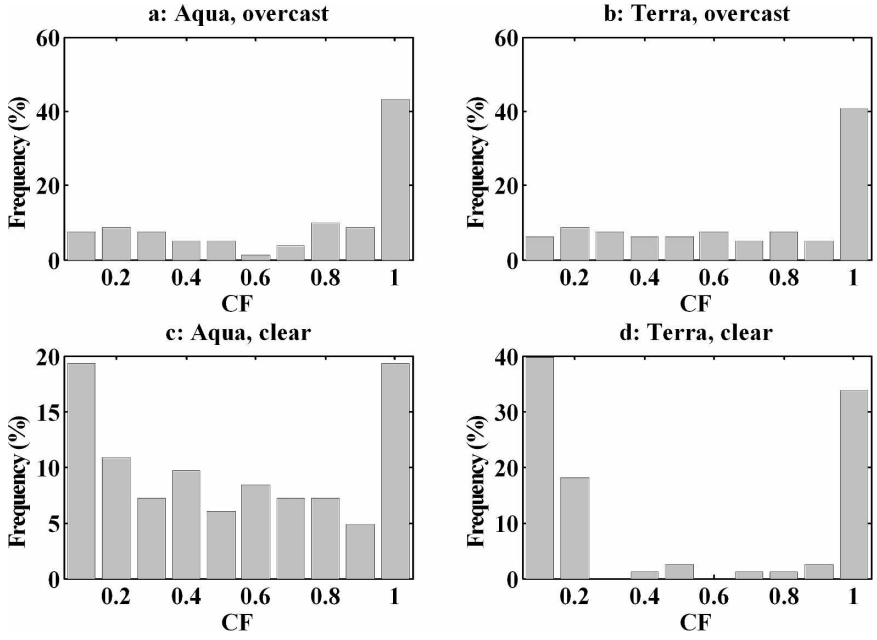

FIG. 4. Cloud fractions from two MODIS datasets under overcast and clear conditions: (top) overcast and (bottom) clear; (left) *Aqua* and (right) *Terra*.

not mean it is better than manobs for comparison with MODIS snapshots. If the ceilometer was used for that purpose, it raises this question: Is this discrepancy caused by the inability of detecting high clouds by ceilometer? Is it possible that the MODIS product is correct, as there could be high clouds above which the ceilometer detection ranges? There is another inevitable inability of the ceilometer to make comparisons with MODIS snapshots. MODIS makes a snapshot of the whole-sky cloud condition above the field site instantly while the ceilometer can only send out a beam to detect cloud covers just above the sensor window. The spatial mismatch is obvious. A solution to this problem is to make a temporal average to both datasets. The temporal average introduces another problem, that is, the mismatch of the sampling objects by ceilometer and MODIS. Ceilometer continuously samples the sky while MODIS has to take a snapshot over the same sky every 90 min. The cloud condition may change significantly during the 90-min gap. Manobs has a big advantage as it can make a snapshot of the all-sky cloud condition instantly. This feather makes it comparable to MODIS. The biggest problem of manobs is the subjectivity in estimating cloud fraction if the sky is neither overcast nor totally clear. Another problem about manobs is that it is difficult to be conducted during the dark night without light. To avoid the first problem, we discarded all of the manobs records if the sky was neither overcast nor totally clear. The second problem is inevitable at the dark winter nights. We admit it as a caveat of this study. But beginning from spring, the solar zenith angle (SZA) was always smaller than 90° between 1300 and 1800 LST, which meant that sunlight was always an available light source for our observations.

We selected 81 clear-sky cases and 83 overcast cases reported by the observer. In each case, the time difference between the two satellites' overpass is shorter than 25 min. According to manobs, the sky condition did not change during the temporal gap. Statistics of the CFs reported by the two MODIS products are shown (Fig. 4).

When the sky is overcast (Figs. 4a,b), both MODIS products have similar results: over 40% of all cases are correctly reported as totally covered (CF = 1) and incorrect reports are almost evenly distributed when CF varies between 0 and 0.9. When the sky is clear (Figs. 4c,d), *Aqua* takes 20% clear-sky cases as overcast and *Terra* over 30%. However, *Terra* MODIS performs better than *Aqua* MODIS according to the frequency distribution of incorrect reports. *Terra* correctly reports almost all of the other clear-sky cases as cloudless or slightly cloudy (CF $\leq$ 0.2) so that the pattern is close to a bimodal distribution (Fig. 4d), which implies that the radiometer on the spacecraft is stable and only the algorithm needs further improvement. Some previous studies (e.g., Hahn et al. 1995) found that in polar areas, meteorological observers tend to underestimate cloud amounts in winter by the availability of moonlight.

Schweiger et al. (2002) concluded that adding the bias (<5%) to the Surface Heat Budget of the Arctic Ocean (SHEBA) observations is insufficient to account for the entire difference. Here, according to Fig. 4d, it is possible that manobs may underestimate the cloud amount by over 10% in winter when the sky is slightly cloudy. The cosine values of solar zenith angles for 3 CF bins ($0 \le CF \le 0.1$, $0.1 < CF \le 0.2$, and $0.9 < CF \le 0.1$) in Fig. 4d are compared in Fig. 5. All of the cases with CF between 0.1 and 0.2 occurred when cos(SZA) < 0.05 (i.e., SZA $> 87°$). The large discrepancies (taking clear sky as overcast; shown as triangles in Fig. 5) occurred when cos(SZA) is between 0.05 and 0.4, indicating that current CF detection algorithms have difficulties in detecting cloud masks with large SZA (e.g., in twilight, over snow-covered backgrounds). When cos(SZA) is larger than 0.4, *Terra* can detect all of the clear-sky events. These results agree very well with recent findings by Frey et al. (2006), who compared cloud fraction statistics between MODIS, Advanced Very High Resolution Radiometer (AVHRR) Polar Pathfinder, and Geoscience Laser Altimeter System (GLAS) products. They concluded that MODIS and the other two datasets agree very well during times of high sun (April–August), almost well during times of low sun (November–February), and the largest discrepancy happened in March. Moreover, they claimed that the largest discrepancy of cloud pattern is located in the Beaufort Sea. Figure 5 seems to indicate that manobs may underestimate CFs in winter polar areas (during darkness) when the sky is slightly cloudy (CF < 0.2). There is a caveat in this conclusion because the actual cloud condition is not available during darkness and both manobs and MODIS may provide an incorrect cloud fraction, which makes our conclusion meaningless. However, the similar findings by Frey et al. (2006) and Schweiger et al. (2002) for cloud detection during Arctic nights lend more credit to our conclusion.

With respect to *Aqua*, results are somewhat different (Fig. 6). We still can see the underestimation of CF according to manobs: all of the cases with CF between 0.1 and 0.2 occurred with small cos(SZA) but it can get as large as 0.15. The algorithm difficulties leading to incorrect reports (taking clear skies as overcast) still occur when cos(SZA) is between 0.1 and 0.4. When it is dark [cos(SZA) < 0], *Aqua* MODIS is extremely variable relative to its *Terra* counterpart. The incorrect CF is almost evenly distributed between 0 and 1. When the SZA is high [cos(SZA) > 0.4], *Aqua* MODIS reports CFs similar to *Terra* MODIS, indicating that the uncertainties caused by the instrument are insignificant.

A possible explanation for the poor performance of *Aqua* MODIS in winter and early spring polar areas is that the *Aqua* 1.6-μm (near-infrared) channel has some dead sensors and the 2.1-μm channel is used as a replacement by some calibration based on the empirical relationship between these two channels (Minnis et al. 2003). The error of such an empirical relationship may become significant when SZA becomes large. Frey et al. (2006) also question the performance of 2.1 μm but they guess that the poor performance may be a result of the contamination by reflectance over snow surface at the near-infrared band (R. Frey 2007, personal communication). More detailed studies are necessary to clarify this.

The time-scale correlations between CFs from two MODIS, NCEP, and manobs are compared (Fig. 7). The conclusion from this study is slightly different from those from previous studies in similar environments (Schweiger et al. 1999, 2002): here the correlation coefficients (CCs) from *Terra* and NCEP only slightly increase with time scales and peak at the 4-day scale with a value of about 0.6, then decrease. According to Schweiger et al. (1999, 2002), the CCs significantly increase when the time scale increases from 1 to 4 days

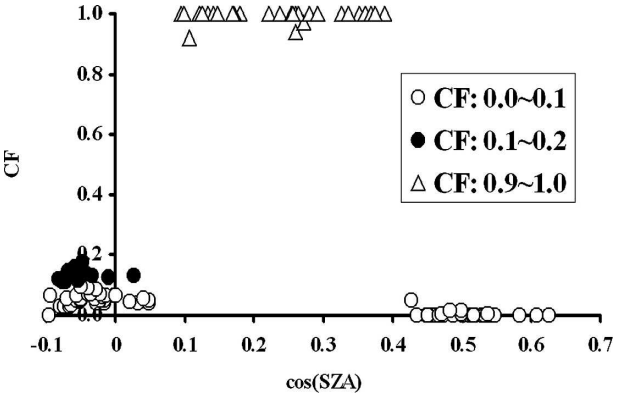

FIG. 5. *Terra* CF distributions with cos(SZA) when the sky is reported as cloudless according to meteorological observers.

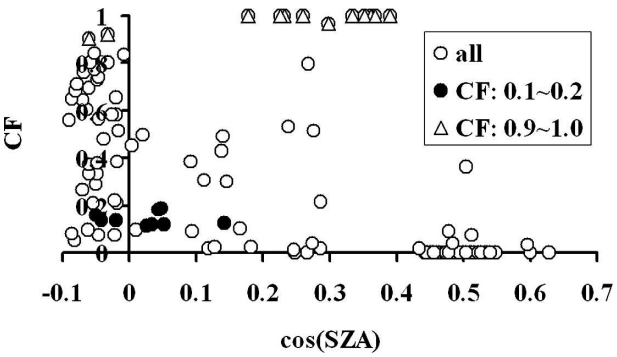

FIG. 6. As in Fig. 5, but for *Aqua*.

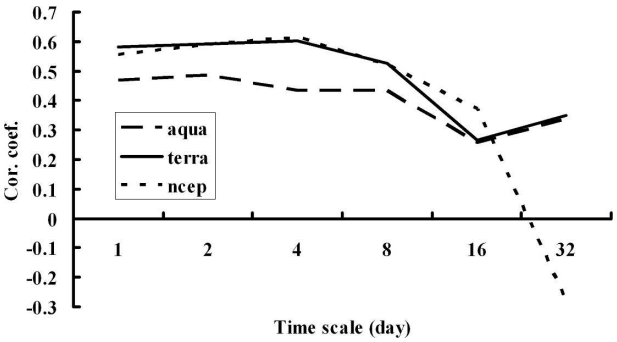

FIG. 7. Correlations between CFs from two MODIS, NCEP, and manobs with different time scales.

and then peak at the 8-day scale. An explanation to the stable CCs when the time scale is smaller than 8 days is that the manobs data in CASES have a much higher sampling frequency than those in the other two studies. During CASES, the surface meteorological observation lasted almost 16 h per day so that the error caused by the temporal discrepancy between satellite- and ground-based observations at short time scales is minimized. During SHEBA the relatively low sampling of 4 times per day and 6 h between two continuous observations made for a more difficult comparison temporally. Taking the ground observation as standard, we can evaluate the qualities of other CF datasets according to Fig. 7. *Terra* and NCEP have similar and better CCs than *Aqua* when the time scale is smaller than 8 days. Considering the poor performance of *Aqua* MODIS in detecting clear skies (Figs. 4c, 6), this conclusion is reasonable. When the time scale is between 8 and 16 days, NCEP has better CCs than the 2 MODIS products though all 3 CCs decrease with increased time scale. The power spectrum analysis and wavelet analysis in the next two sections will help to explain this phenomenon. When the time scale is ≥16 days, the 2 MODIS products have similar and better CCs (between 0.3 and 0.4) than NCEP, showing the disadvantages of NCEP in predicting mid- and long-term CF evolutions. However, the pattern shown in Fig. 7 is not very certain when the time scale is more than 16 days because the sampling number is too small (e.g., there are only 8 samples when the time scale is 32). Further studies with larger sampling numbers are necessary.

b. Power spectrum analysis

The power spectrums of these five CF time series are plotted (Fig. 8). Taking the manobs (Fig. 8d) as standard, the CF time series over the experimental site has two active periods: one is between 2 and 4 days, and another is slightly beyond 8 days (more precisely, 9.1 days). *Terra* catches both of these periodicities (Fig. 8b), though both are weaker than those detected with manobs. Thus, the algorithm for detecting clear skies from snow-covered backgrounds with large SZAs is the main reason for the weakening in the periodicity of *Terra* CF time series. *Aqua* can detect these two periodicities as well but both of them have weaker power than those revealed by *Terra*. According to Fig. 4c and Fig. 6, we can say that the algorithm issues result in the poor performance of *Aqua* MODIS in detecting clear skies in winter and early spring over snow-covered backgrounds, which leads to a weakening in the periodicity of its CF time series and leads to the smaller CC at most time scales (Fig. 7). NCEP (Fig. 8c) successfully

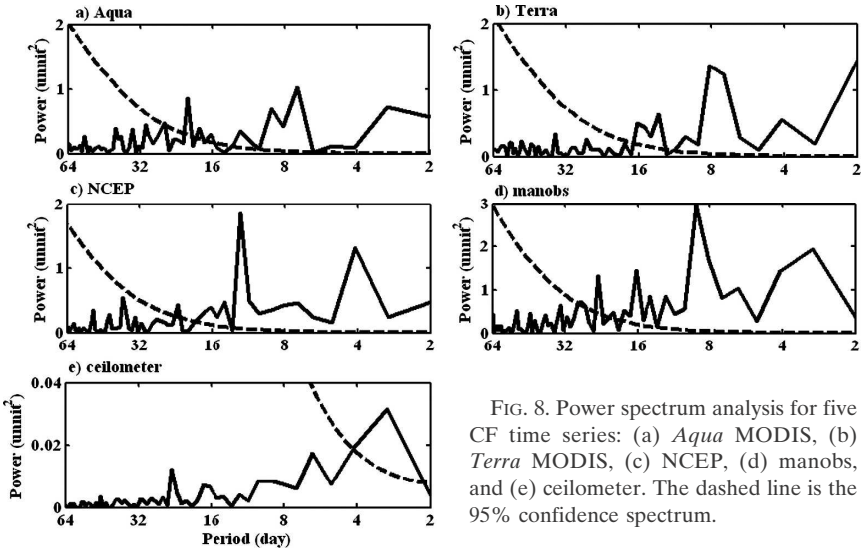

FIG. 8. Power spectrum analysis for five CF time series: (a) *Aqua* MODIS, (b) *Terra* MODIS, (c) NCEP, (d) manobs, and (e) ceilometer. The dashed line is the 95% confidence spectrum.

predicts the periodicity around the 4-day scale but has a significant phase lag in predicting the period around the 8-day scale. More precisely, the NCEP data peak at the 12.2-day periodicity, which is 3 days later than manobs. Comparing the periodicities in these four figures (8a–d) can explain the patterns in Fig. 7. According to Fig. 8e, the ceilometer can only represent the period between 2 and 4 days, showing that middle and low clouds are more active within this period. Since there exists a significant period around the 8-day scale according to manobs, it is believable that high clouds have stronger links to synoptic events while middle and low clouds may be generated by more local influences and processes.

c. *Wavelet analysis*

The wavelet analysis of CF time series can detect not only the periodicities of this series but also the temporal evolution of such periodicities. The wavelet analysis of these five CF time series is shown (Fig. 9). In mid- and late spring (April and May), the cloud cover is active with periods between 2 and 4 days (Figs. 9a,b). CFs from the two MODIS products and the ceilometer support this conclusion. Still, the ceilometer can prove that such variability is controlled by low and middle clouds (Fig. 9e). However, we do not get the same conclusion from either the manobs CF series or the NCEP CF series. The reasons, however, are different for each case. Referring to Fig. 3, we see that NCEP does not simulate the quick increase of cloud amount in spring. The lack of knowledge in simulating MPACs makes it impossible to get the correct CF wavelet spectrum in spring. According to manobs, the periodic property of CF time series in winter and spring is dominant with the periodicity between 8 and 16 days, which is located in midwinter (December and January). The power of the periodicity between 2 and 4 days is much weaker (Fig. 8d), although the absolute value of the power of this period is larger than that detected with either MODIS or the ceilometer. The periodicity between 8 and 16 days in midwinter can be detected not only with manobs and NCEP but *Terra* MODIS can detect it as well (Fig. 9b).

4. Conclusions

In this study, we have evaluated the quality of daily averaged CF time series collected from different platforms: two MODIS instruments on the *Terra* and *Aqua* satellites, the NCEP reanalysis data, a ceilometer, and manobs over landfast first-year sea ice during the CASES over the wintering experiment. According to these independent datasets, we conclude the following:

1) The temporal evolution of CF in CASES is similar to that observed in previous studies. It has a significant seasonal variation in April. However, the NCEP products cannot capture the seasonality of CF in the Arctic spring. It significantly underestimated CFs in spring (e.g., from April to May) and cannot predict the quick increase of CFs from about 0.3 to 0.75. Both MODIS products overestimated CFs in February and March. In winter (December–February), *Aqua* MODIS significantly overestimated CFs relative to *Terra* MODIS (*Terra* was more similar to manobs). Case study analysis shows that *Aqua* MODIS misrepresents the snow-covered surface as clouds during the dark winter [$\cos(\mathrm{SZA}) < 0$]. When $0.1 < \cos(\mathrm{SZA}) < 0.4$, both MODIS products tend to misrepresent the snow-covered background as clouds, leading to the overestimate of CFs in late winter (February) and early spring (March). When cos(SZA) is larger than 0.4, both MODIS products have good performance in detecting cloud masks over snow backgrounds.
2) Manobs tends to underestimate cloud masks during partly cloudy skies during darkness. Comparing the CFs from *Terra* and manobs, we conclude that this bias can be near 10%. However, this does not affect the manobs-derived CF periodicity in the winter Arctic when compared with the *Terra* dataset.
3) High clouds appear more frequently in winter than in spring according to manobs and the ceilometer; however, this could be the result of not being able to see or detect high clouds when low- and mid-level clouds become more abundant in spring. In winter, if high clouds are included in the analysis, the total CF shows periods between 8 and 16 days according to the spectral analysis, which may indicate their close connection with synoptic events. Current NCEP products can predict this periodicity but with a phase lag of 3 days. Middle and low clouds can be generated by local forcings (e.g., topography and open water) and are common in mid- and late spring (April and May), and the total CF in this stage, no matter whether high clouds are included or not, has periods between 2 and 4 days. More in-depth climatologies of Arctic cloud types may be possible during the upcoming CloudSat mission.
4) The time-scale-dependent CCs between both MODIS products, NCEP and manobs, show that with high-frequency CF sampling per day, the CCs are stable when the time scale varies between 1 and 4 days (with *Terra* MODIS and NCEP, the value is about 0.6; with *Aqua* MODIS, it is between 0.4 and 0.5). When the time scale increases beyond 8 days, all CCs get smaller—those from the two MODIS

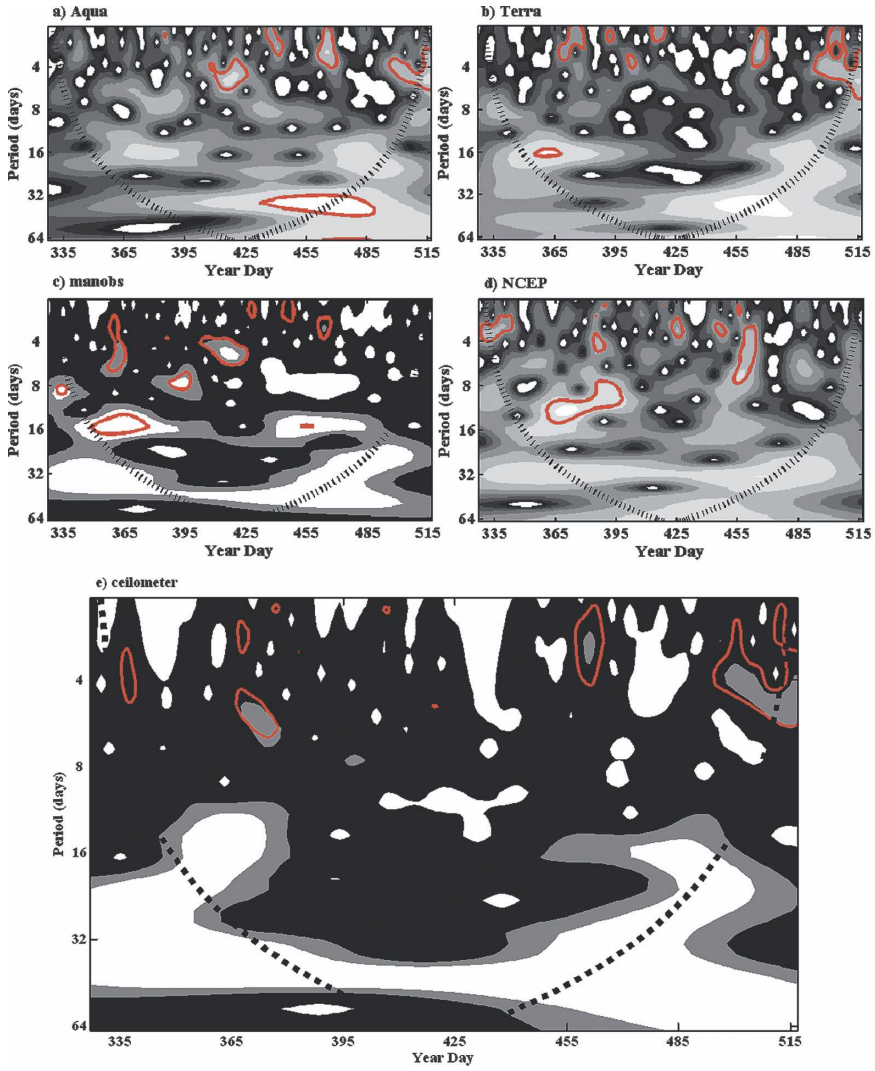

FIG. 9. The wavelet power spectrum of the CF time series from five sources: (a) *Aqua* MODIS, (b) *Terra* MODIS, (c) manobs, (d) NCEP, and (e) ceilometer. The x axis is the yearday (YD; starting from 1 Jan 2003) between YD 327 (22 Nov 2003) and YD 517 (31 May 2004). In each panel, the power has been scaled by the global wavelet spectrum, and the region outlined by the hatched line is the cone of influence, where zero padding has reduced the variance to a level where interpretation of the significance of these periods is questionable (i.e., outside the cone). The method to determine the edge effect is from Torrence and Compo (1998). The red contour is the 5% significance level, using a red noise background spectrum.

products agree more closely with values between 0.3 and 0.4, and those from NCEP dramatically decrease from positive values to negative values, indicating the lack of accuracy in current NCEP cloud schemes.

Acknowledgments. This study was funded by the Natural Science and Engineering Research Council, the ArcticNet networks Centres of Excellence, and the Northern Studies Training Program (NSTP). The authors acknowledge the field observations by An Tat, Jim Butler, and Teresa Fisico, all of whom are graduate students at the Centre for Earth Observation Science (CEOS), University of Manitoba. The authors also thank the crew of the CCGS Amundsen for logistical support during the CASES project.

REFERENCES

Ackerman, S. A., K. I. Strabala, W. P. Menzel, R. A. Frey, C. C. Moeller, and L. E. Gumley, 1998: Discriminating clear sky from clouds with MODIS. *J. Geophys. Res.,* **103,** 32 141–32 158.

Chen, Y., J. A. Francis, and J. R. Miller, 2002: Surface temperature of the Arctic: Comparison of TOVS satellite retrievals with surface observations. *J. Climate,* **15,** 3698–3708.

Curry, J. A., and E. E. Ebert, 1992: Annual cycle of radiation fluxes over the Arctic Ocean: Sensitivity to cloud optical properties. *J. Climate,* **5,** 1267–1280.

——, W. B. Rossow, D. Randall, and J. L. Schramm, 1996: Overview of Arctic cloud and radiation characteristics. *J. Climate,* **9,** 1731–1764.

Frey, R., M. J. Pavlonis, and J. Key, 2006: Comparison of polar cloud cover statistics between MODIS, AVHRR Pathfinder, and GLAS. Preprints, *12th Conf. on Atmospheric Radiation,* Madison, WI, Amer. Meteor. Soc., CD-ROM, P4.30.

Fu, Q., and S. Hollars, 2004: Testing mixed-phase cloud water vapor parameterizations with SHEBA/FIRE–ACE observations. *J. Atmos. Sci.,* **61,** 2083–2091.

Hahn, C. J., S. G. Warren, and J. London, 1995: The effect of moonlight on observation of cloud cover at night, and application to cloud climatology. *J. Climate,* **8,** 1429–1446.

Hanesiak, J., 1998: Ice camp meteorological observations. *NOW '98 Sea Ice/Climate Dynamic Subgroup Field Summary,* T. N. Papakyriakou, C. J. Mundy, and D. G. Barber, Eds., Centre for Earth Observation Science, Geography Department, University of Manitoba, CEOS Tech. Rep. 98-8-2, 21–32.

Intrieri, J., C. Fairall, M. Shupe, P. Persson, E. Andreas, P. Guest, and R. Moritz, 2002: An annual cycle of Arctic surface cloud forcing at SHEBA. *J. Geophys. Res.,* **107,** 8039, doi:10.1029/2000JC000439.

Key, E. L., P. J. Minnett, and R. A. Jones, 2004: Cloud distributions over the coastal Arctic Ocean: Surface-based and satellite observations. *Atmos. Res.,* **72,** 57–88.

Li, Z., M. C. Cribb, F.-L. Chang, and A. P. Trishchenko, 2004: Validation of MODIS-retrieved cloud fractions using whole-sky imager measurements at the three ARM sites. *Proc. 14th ARM Science Team Meeting,* Albuquerque, NM, U.S. Department of Energy. [Available online at http://www.arm.gov/publications/proceedings/conf14/extended_abs/li1-z.pdf.]

Lindsay, R. W., D. B. Percival, and D. A. Rothrock, 1996: The discrete wavelet transform and the scale analysis of the surface properties of sea ice. *IEEE Trans. Geosci. Remote Sens.,* **34,** 771–787.

Liu, Y., J. R. Key, R. A. Frey, S. A. Ackerman, and W. P. Menzel, 2004: Nighttime polar cloud detection with MODIS. *Remote Sens. Environ.,* **92,** 181–194.

Minnett, P. J., 1999: The influence of solar zenith angle and cloud type on cloud radiative forcing at the surface in the Arctic. *J. Climate,* **12,** 147–158.

Minnis, P., D. F. Young, S. Sun-Mack, P. W. Heck, D. R. Doelling, and Q. Z. Trepte, 2003: CERES cloud property retrievals from imagers on TRMM, *Terra,* and *Aqua. Remote Sensing of Clouds and the Atmosphere VIII,* K. P. Schaefer et al., Eds., International Society for Optical Engineering (SPIE Proceedings Vol. 5235), 37–48.

Schweiger, A. J., 2004: Changes in seasonal cloud cover over the Arctic seas from satellite and surface observations. *Geophys. Res. Lett.,* **31,** L12207, doi:10.1029/2004GL020067.

——, R. W. Lindsay, J. R. Key, and J. A. Francis, 1999: Arctic clouds in multiyear satellite data sets. *Geophys. Res. Lett.,* **26,** 1845–1848.

——, ——, J. A. Francis, J. Key, J. M. Intrieri, and M. D. Shupe, 2002: Validation of TOVS Path-P data during SHEBA. *J. Geophys. Res.,* **107,** 8041, doi:10.1029/2000JC000453.

Shupe, M. D., T. Uttal, and S. Y. Matrosov, 2005: Arctic cloud microphysics retrievals from surface-based remote sensors at SHEBA. *J. Appl. Meteor.,* **44,** 1544–1562.

Torrence, C., and G. P. Compo, 1998: A practical guide to wavelet analysis. *Bull. Amer. Meteor. Soc.,* **79,** 61–78.

Walsh, J. E., and W. L. Chapman, 1998: Arctic cloud–radiation–temperature associations in observational data and atmospheric reanalyses. *J. Climate,* **11,** 3030–3045.

Zuidema, P., and Coauthors, 2005: An Arctic springtime mixed-phase cloudy boundary layer observed during SHEBA. *J. Atmos. Sci.,* **62,** 160–176.